

Development of a Prolonged Calcium Plateau in Hippocampal Neurons in Rats Surviving Status Epilepticus Induced by the Organophosphate Diisopropylfluorophosphate

Laxmikant S. Deshpande,* Dawn S. Carter,* Robert E. Blair,* and Robert J. DeLorenzo*^{†,‡,1}

*Department of Neurology, †Department of Pharmacology and Toxicology, and ‡Department of Molecular Biophysics and Biochemistry, Virginia Commonwealth University, Richmond, Virginia 23298

¹To whom correspondence should be addressed at School of Medicine, Virginia Commonwealth University, PO Box 980599, Richmond, VA 23298. Fax: (804) 828-6432. E-mail: rdeloren@vcu.edu.

Received April 8, 2010; accepted May 15, 2010

Organophosphate (OP) compounds are among the most lethal chemical weapons ever developed and are irreversible inhibitors of acetylcholinesterase. Exposure to majority of OP produces status epilepticus (SE) and severe cholinergic symptoms that if left untreated are fatal. Survivors of OP intoxication often suffer from irreversible brain damage and chronic neurological disorders. Although pilocarpine has been used to model SE following OP exposure, there is a need to establish a SE model that uses an OP compound in order to realistically mimic both acute and long-term effects of nerve agent intoxication. Here we describe the development of a rat model of OP-induced SE using diisopropylfluorophosphate (DFP). The mortality, behavioral manifestations, and electroencephalogram (EEG) profile for DFP-induced SE (4 mg/kg, sc) were identical to those reported for nerve agents. However, significantly higher survival rates were achieved with an improved dose regimen of DFP and treatment with pralidoxime chloride (25 mg/kg, im), atropine (2 mg/kg, ip), and diazepam (5 mg/kg, ip) making this model ideal to study chronic effects of OP exposure. Further, DFP treatment produced N-methyl-D-aspartate (NMDA) receptor-mediated significant elevation in hippocampal neuronal $[Ca^{2+}]_i$ that lasted for weeks after the initial SE. These results provided direct evidence that DFP-induced SE altered Ca^{2+} dynamics that could underlie some of the long-term plasticity changes associated with OP toxicity. This model is ideally suited to test effective countermeasures for OP exposure and study molecular mechanisms underlying neurological disorders following OP intoxication.

Key Words: OPs; SE; DFP; mortality; EEG; calcium dynamics; Sprague-Dawley rats.

The attacks of 11 September 2001 in United States illustrate the willingness of terrorists to use any means of weapons to induce mass civilian casualties. Organophosphate (OP) compounds such as soman, sarin, tabun, and O-ethyl S-[2-(diisopropylamino)ethyl] methylphosphonothioate are chemical warfare nerve agents known to produce lethal toxicities and death (Coupland and

Leins, 2005). The potential of being exposed to the nerve agents exists on the battlefields (Reviewed In: Newmark, 2004) and also to the civilian population as a terrorist threat (Yokoyama *et al.*, 1996) or acts of war (Dingeman and Jupa, 1987). In addition, some OP compounds are also used as insecticides and therefore represent a major public health concern (Eyer, 2003; Karaliedde and Senanayake, 1989). Thus, it is important to study effects of chemical/biological warfare agents and develop effective countermeasures in order to limit mortality and ensuing physical and mental damage.

OP compounds/nerve agents are irreversible inhibitors of cholinesterase enzyme, particularly acetylcholinesterase (AChE) (Bajgar, 2004). Inhibition of AChE results in rapid buildup of acetylcholine at synapses causing a hypercholinergic crisis. One of the major symptoms of increased synaptic acetylcholine levels is the expression of status epilepticus (SE). These cholinergic symptoms if left untreated are life threatening (McDonough and Shih, 1997; Shih *et al.*, 2003). Subjects who survive nerve agent-induced SE develop irreversible brain damage (Lemerrier *et al.*, 1983) and may have chronic health problems (Golomb, 2008). Further, SE survivors suffer from epilepsy, depression, and cognitive deficits (Rod, 2009). However, the mechanisms underlying development and expression of these chronic neurological disorders following OP toxicity are still unknown (Mark and Kelley 1998).

Because SE is a major cause of the neurological injury following OP toxicity, animal models of SE have been used to investigate OP injury. Administration of cholinergic agonist pilocarpine produces SE in animals and is a widely used model to induce convulsions and study epilepsy in the laboratory (Turski *et al.*, 1983) and has also been used to mimic seizures following nerve agent exposure (Tetz *et al.*, 2006). However, there is a pressing need to establish a SE model that uses an OP agent in order to realistically model both acute and long-term effects of nerve agent intoxication. Such a model requires a good survival rate and would be immensely helpful in developing

pharmacological agents and therapies for treatment of pathologies associated with OP toxicity (Broomfield and Kirby, 2001).

The prototypical OP compound diisopropylfluorophosphate (DFP) has been employed to model seizures and convulsions in rodents (Auta *et al.*, 2004; Bouzarth and Himwich, 1952; Wright *et al.*, 2009). DFP renders AChE resistant to hydrolysis, inactivating the enzyme resulting in cholinergic crises and ultimately death (McDonough and Shih, 1997). Although DFP is not a gas that has been weaponized for mass effect, if it is administered parenterally its effects are identical to other nerve agents in its ability to irreversibly inhibit AChE and produce seizures, irreversible brain damage, and a very high mortality rate if not aggressively treated. DFP is a safer OP compound to handle; therefore, it is an ideal candidate for a model of SE and investigating chronic neurological disorders resulting from nerve agent exposure.

Research from our laboratory has demonstrated that many of the long-term effects of SE on producing acquired epilepsy and cognitive impairment are mediated by a prolonged rise in intracellular calcium levels $[Ca^{2+}]_i$ termed the Ca^{2+} plateau (Raza *et al.*, 2004). Thus, studying Ca^{2+} dynamics following OP exposure may offer a unique insight into the pathophysiology of OP-induced toxicity. This study was initiated to develop a model of DFP toxicity that produces SE and has a high survival rate in order to investigate the electroencephalogram (EEG) characteristics and the $[Ca^{2+}]_i$ dynamics in acutely isolated hippocampal neurons for up to a month after DFP exposure. The results demonstrate that the behavioral manifestations and EEG profile for DFP-induced seizures were similar to those reported for nerve agents (McDonough and Shih, 1993; Shih *et al.*, 2003) and provide the first high-resolution electrophysiology characterization of DFP-induced SE. Significantly, higher survival rates could be obtained with an improved dose regimen consisting of pralidoxime chloride (2-PAM), atropine, and diazepam, providing a useful model to investigate Ca^{2+} dynamics following OP exposure. DFP treatment produced significant elevation in $[Ca^{2+}]_i$ levels (calcium plateau) that lasted for weeks after the initial seizure. This Ca^{2+} entry was mediated by N-methyl-D-aspartate (NMDA) receptor system. These results provide direct evidence that DFP-induced SE alters Ca^{2+} dynamics and suggest that this significant change in $[Ca^{2+}]_i$ levels could underlie some of the long-term plasticity changes associated with nerve agent toxicity.

MATERIALS AND METHODS

Animals. All animal use procedures were in strict accordance with the National Institute of Health Guide for the Care and Use of Laboratory Animals and approved by Virginia Commonwealth University's Institutional Animal Care and Use Committee. Male Sprague-Dawley rats (Harlan, Indianapolis, IN) weighing 250–300 g were used in this study. Animals were housed two per cage at 20–22°C with a 12 light:12 dark hour cycle (lights on 0600 to 1800 h) and free access to food and water.

Chemicals. All the chemicals were obtained from Sigma Aldrich Company (St. Louis, MO) unless otherwise noted. DFP was supplied as an oily solution which was dissolved in ice-cold PBS just before the experiment

and injected subcutaneously (sc). All other drugs, pyridostigmine bromide, atropine sulfate, pralidoxime chloride (2-PAM), and ([+]-5-methyl-10,11-dihydro-5H-dibenzo[a,d] cyclohepten-5,10-imine maleate) (MK-801), were dissolved in saline (0.9% NaCl). Diazepam was obtained from Virginia Commonwealth University health system pharmacy. DFP was always prepared fresh and kept on ice until the time of injections. Stocks for all other drugs were kept for no more than 3 weeks under the prescribed storage conditions.

Electrode implantation and seizure monitoring. Rats were stereotaxically implanted with three skull surface electrode screws with teflon-insulated stainless steel wire (Plastics One, Roanoke, VA) under general anesthesia with isoflurane (5%). Electrode screws were positioned through burr holes above the right and left frontal cortices (anteroposterior, 3 mm, and mediolateral, ± 3 mm from bregma); the third surface electrode screw was positioned over the cerebellum to serve as reference, and two additional (nonelectrode) skull screws were inserted for structural support. The electrode screws were seated to contact but not penetrate the dura mater. Female amphenol terminals connected to the electrode wire were seated into an electrode pedestal (Plastics One), and this assembly was secured to the skull with Cerebond adhesive (Plastics One). Rats were allowed 1 week of recovery time before the start of the experiment. Wire leads were securely connected into the threaded electrode pedestal on the rat and then connected to an electrical-swivel commutator (Plastics One) to allow for free movement of the rat while maintaining continuity of EEG signals. EEG signals were amplified using a Grass model 8-10D (Grass Technologies, West Warwick, RI) and digitized with Powerlab 16/30 data acquisition system (AD Instruments, Colorado Springs, CO). Evaluation of digitally acquired EEG was performed with Labchart (AD Instruments).

DFP-induced SE. All the animals received pretreatment with pyridostigmine bromide (0.026 mg/kg, im) 30 min before DFP injection. One minute following DFP injection, animals received 2-PAM (25 mg/kg, im) and atropine (2 mg/kg, ip). These treatments approved by the Food and Drug Administration are employed by U.S. Army as countermeasures against nerve gas intoxication (Broomfield and Kirby, 2001; Golomb, 2008). Rats underwent convulsions and SE-like activity within 7–10 min following DFP. Behavioral observations and Racine scores were made (see Table 3). If the animals went into SE and survived 1 h of seizure activity, they were injected with diazepam (5 mg/kg, ip) and 2-PAM (25 mg/kg, im) at 1, 3, and 5 h following SE onset to terminate and control seizures. Sham animals received all the drugs except for DFP at the same time as the DFP-treated animals. Sham animals did not experience any convulsions or seizure-like activity. For NMDA studies, animals were injected with MK-801 (4 mg/kg, ip) 30 min prior to DFP injection. Surviving animals were then injected with saline and fed lactose milk as part of supportive care and returned to home cage. For Ca^{2+} studies, animals were sacrificed at 1 h following SE onset or at 1, 2, 7, 14, or 30 days after SE. Mortality was assessed at 24 h.

Isolation of hippocampal CA1 neurons and loading with Fura-2. Acute isolation of CA1 hippocampal neurons was performed by established procedures (Raza *et al.*, 2004). Animals were anesthetized with isoflurane and decapitated. Brains were rapidly dissected and placed in 4°C oxygenated (95/5%) artificial cerebrospinal fluid (aCSF) consisting of (in mM) 120 NaCl, 25 glucose, 20 PIPES, 5 KCl, 7 $MgCl_2$, and 0.1 $CaCl_2$. Slices were then treated with 8 mg/ml protease in PIPES-aCSF for 6 min at 34°C and rinsed. Slices were visualized on a dissecting microscope, and the CA1 hippocampal layer was excised. The removed CA1 regions were triturated with a series of Pasteur pipettes of decreasing diameter in cold (4°C) PIPES-aCSF solution containing 1 μM Fura-2 AM (Invitrogen, Carlsbad, CA). The cell suspension was placed in the middle of two well glass-bottomed chambers. These glass chambers were previously treated overnight with 0.05 mg/ml poly-L-lysine followed by multiple rinses with distilled water and then further treated with Cell-Tak

(BD-Biosciences, San Jose, CA) biocompatible cellular adhesive (3.5 $\mu\text{g}/\text{cm}^2$) for 1 h, rinsed, and air dried. Neuronal suspension placed in the center of adhesive coated dishes when settled firmly adhered to the bottom. This technique simplified further manipulations on the dissociated neurons. Plates were placed in a humidified oxygenated chamber at 37°C for 1 h. Fura-2 was washed off with PIPES-aCSF and incubated an additional 15 min to allow for complete cleavage of the AM moiety from Fura-2.

Measurement of $[\text{Ca}^{2+}]_i$. Fura-2 loaded cells were transferred to a 37°C heated stage (Harvard Apparatus, Hollington, MA) on an Olympus IX-70 inverted microscope coupled to a fluorescence imaging system (Olympus America, Center Valley, PA) and subjected to $[\text{Ca}^{2+}]_i$ measurements by procedures well established in our laboratory (Raza *et al.*, 2004). All experiments were performed using a 20 \times , 0.7 N.A. water-immersion objective, and images were recorded by an ORCA-ER high-speed digital CCD camera (Hamamatsu Photonics K.K., Japan). Fura-2 was excited with a 75-W xenon arc lamp (Olympus America). Ratio images were acquired by alternating excitation wavelengths (340/380 nm) by using a Lambda 10-2 filter wheel (Sutter Instruments Co., Novato, CA) and a Fura filter cube at 510/540 emission with a dichroic at 400 nm. All image acquisition and processing were controlled by a computer connected to the camera and filter wheel using Metafluor Software ver 7.6 (MDS Analytical Technologies, Downingtown, PA). Image pairs were captured every 5 s, and the images at each wavelength were averaged over 10 frames. Background fluorescence was obtained by imaging a field lacking Fura-2.

Calcium calibration. We performed Ca^{2+} calibration determinations as described previously (Raza *et al.*, 2004) to provide estimates of absolute $[\text{Ca}^{2+}]_i$ concentrations from the 340/380 ratio values. A Ca^{2+} calibration curve was constructed using solutions of calibrated Ca^{2+} buffers ranging from 0 Ca^{2+} (Ca^{2+} free) to 39 μM Ca^{2+} (Invitrogen). Values from the calibration curve were used to convert fluorescent ratios to $[\text{Ca}^{2+}]_i$. Final $[\text{Ca}^{2+}]_i$ were calculated from the background corrected 340/380 ratios using the following equation (Grynkiewicz *et al.*, 1985):

$$[\text{Ca}^{2+}]_i = (K_d \times Sf_2/Sb_2) \times (R - R_{\min}) / (R_{\max} - R),$$

where R is the 340/380 ratio at any time; R_{\max} is the maximum measured ratio in saturating Ca^{2+} solution (39 μM free Ca^{2+}); R_{\min} is the minimal measured ratio Ca^{2+} free solution; Sf_2 is the absolute value of the corrected 380-nm signal at R_{\min} ; Sb_2 is the absolute value of the corrected 380-nm signal at R_{\max} ; and the K_d value for Fura-2 is 224 nM.

Data analysis. For comparison of $[\text{Ca}^{2+}]_i$ between sham and DFP-treated animals, ratios were normalized to percent of control values. Student's t -test or ANOVA was applied when appropriate to compare $[\text{Ca}^{2+}]_i$. The Tukey test was used for all *post hoc* comparisons. For comparing the distributions of $[\text{Ca}^{2+}]_i$ levels, a chi-square test was used. Statistical tests were run using SigmaStat 2.0 and graphs generated with SigmaPlot 8.0 (SPSS Inc., Chicago, IL). $p < 0.05$ was considered statistically significant for all data analysis. We used five to nine animals for each experimental condition or time point studied. Dissociating the hippocampal slices routinely yielded 15–20 healthy, phase-bright neurons that were used for the recordings. The means of each group of neurons from each animal were used to evaluate results and conduct statistical analysis. Viable neurons included in the study had a smooth surface and a pyramidal-like morphology with processes. Nonviable neurons were swollen or circular, and the surface was uneven and irregular. Data from each animal were pooled together in respective groups and ultimately represented as total number of cells studied.

RESULTS

Optimization of Factors Altering Effects of DFP

As shown in Table 1, the ability of DFP to induce seizures and mortality was greatly affected by the vehicle and dose of

TABLE 1
Factors Altering Effects of DFP Administration

Dose of DFP (mg/kg, sc)	Vehicle	Seizures	Mortality
2 and 4	Saline	Yes	100
2 and 4	Peanut oil	No	0
2 and 4	Ice-cold PBS	Yes	50 and 80
2 and 4	Ice-cold PBS	Yes	0 and 10 with 2 mg/kg atropine

DFP and also by the dose of atropine. We initially started out with 2 mg/kg of DFP and increased the DFP dose to 4 mg/kg if no seizures were observed and determined the corresponding mortality. These doses were selected on the basis of published studies on DFP-induced seizures (Pibiri *et al.*, 2008; Tuovinen, 2004; Wright *et al.*, 2009).

The effects of DFP were greatly affected by choice of vehicle. DFP when dissolved in saline was extremely lethal and resulted in 100% mortality at 2 mg/kg dose. DFP when dissolved in peanut oil was ineffective and failed to induce seizures even at 4 mg/kg dose. However, some cholinergic signs including minor salivation and defecation were noted. In some animals, infrequent tremors were also observed. In contrast, DFP when dissolved in ice-cold PBS produced seizures in all the animals and displayed dose-dependent mortality. This vehicle was therefore selected for all the subsequent experiments.

The effects of DFP were also altered by volume of injection. Injection volumes of less than 250 μl resulted in random variability of seizures whereas doses higher than 300 μl produced greater toxicities and death. Such a volume-dependent effect of DFP could be because of kinetics of DFP distribution. We observed reliable seizures in majority of animals with reduced mortalities at a volume of 300 μl , and this injection volume was therefore used for all subsequent experiments.

Finally, the mortality following DFP-induced seizures was also significantly affected by the dose of atropine. A low dose of atropine (0.2 mg/kg, ip) following 2 and 4 mg/kg DFP administration resulted in mortalities of approximately 50%. Increasing the dose of atropine (2 mg/kg, ip) largely attenuated mortality and significantly improved survival rates. Atropine at a higher dose did not prevent the animals from undergoing SE, but effectively blocked the toxic effects of DFP in producing mortality. This higher dose of atropine was therefore used in all the subsequent experiments.

DFP-Induced Seizures and Mortality

After optimizing the vehicle, volume of injection and dose of atropine, we next investigated the dose-dependent effects of DFP on seizures and mortality. As shown in Table 2, DFP doses of 2.5 mg/kg and below had very little mortality, but at these doses seizure induction was unreliable and at best was 50%. At 5 and 10 mg/kg DFP, 100% of the animals displayed

TABLE 2
Dose-Dependent Effects of DFP on Seizure and Mortality

Dose of DFP (mg/kg, sc) in ice-cold PBS	% Animals displaying seizures	% Mortality (atropine: 2 mg/kg, ip)
1	10	0
2	30	0
2.5	50	5
4	90	10
5	100	80
10	100	90

SE, but these doses were associated with extremely high mortality rates. At the 4 mg/kg DFP dose, we observed a very high percentage of animals undergoing SE with significantly lower rates of mortality. DFP had a very narrow dose range for exhibiting seizures with greater survivability. We therefore chose 4 mg/kg dose of DFP for all the subsequent experiments.

DFP had a very quick onset of action. Within 2–3 min of injections, hypercholinergic effects were observed characterized by salivation, urination, defecation, tremors, and wet-dog shakes. Within 5–8 min, seizures were observed and characterized by myoclonic jerks and convulsions that quickly evolved into nonstop seizure activity (SE) that did not abate until we initiated anticonvulsant treatment with sequential diazepam injections at 1 h after initiation of SE. This model provided the ability to produce DFP-induced SE for a standardized period of time. The Racine scores (Racine, 1972) for DFP-induced seizures are given in Table 3. Animals displayed class 5 seizures within 6–8 min.

EEG Characterization of DFP-Induced SE

DFP-induced seizures were also confirmed with EEG recordings. Baseline EEG was recorded for 30 min before DFP injection, and a representative recording is shown in Figure 1A (top trace). DFP onset was very rapid, and the tonic-clonic seizure activity occurred in parallel with high rhythmic EEG activation as shown in Figure 1B. Within 7–8 min, animals progressed into electrographic SE. The SE was intense,

TABLE 3
Racine Scores to Evaluate Behavioral Seizures Following DFP Administration

Time of onset (min)	Behavioral signs	Racine score
2.2 ± 0.2	SLUD	1
3.4 ± 0.3	Tremors, wet-dog shakes	2
5 ± 0.4	Forelimb clonus	3
	Rearing of torso	4
6.8 ± 0.5	Forelimb and hindlimb clonus, rearing and falling back	5

Note. SLUD = salivation, lacrimation, urination, and defecation.

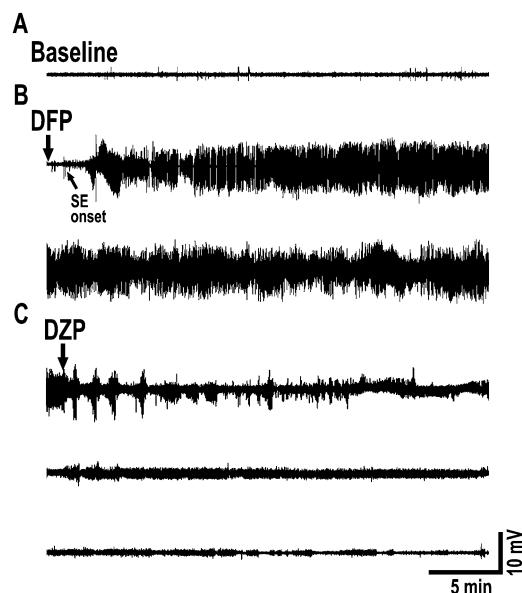


FIG. 1. EEG seizure activity evoked by DFP. (A) Baseline activity before administration of DFP. (B) Onset of DFP action is rapid producing rhythmic high-amplitude and high-frequency spike activity that rapidly progresses into electrographic SE. SE is robust, intense, and does not wax and wane for the entire 1 h. The two traces in panel B together represents one full hour of electrographic SE. (C) Seizures are terminated with diazepam (DZP) injections at 1, 3, and 5 h following onset of SE. These treatments completely stop EEG epileptiform activity. The three traces in panel C represent EEG activity following the three diazepam injections. Traces are representative of $n = 6$ animals.

did not wax or wane, and did not lose its intensity throughout the 1 h of seizure activity (Fig. 1B). Animals were injected with diazepam and 2-PAM injections at 1, 3, and 5 h following onset of SE. This completely terminated both behavioral and electrographic SE (Fig. 1C).

The electrophysiological progression of DFP-induced SE is depicted in Figure 2. EEG alterations following DFP administration were rapid and correlated with behavioral seizure manifestations. Figure 2A shows a baseline EEG recording before DFP injection. Low-voltage fast activity started to appear with 2–3 min of DFP administration (Fig. 2B). High-voltage slow activity (Fig. 2C) appeared within the next minute and rapidly progressed into high-voltage spiking correlating with behavioral seizure activity by approximately 5–6 min (Fig. 2E). By this time, animals were in electrographic SE with fully developed seizures. The seizures continue unabated for 1 h at the end of which they are terminated using diazepam. The EEG pattern for SE termination following diazepam is shown in Figure 1C.

DFP-Induced SE Caused Elevations in Hippocampal Neuronal $[Ca^{2+}]_i$

To investigate if DFP treatment caused long-lasting changes in hippocampal neuronal $[Ca^{2+}]_i$, we measured neuronal $[Ca^{2+}]_i$ after 1 h of SE using the high-affinity, ratiometric

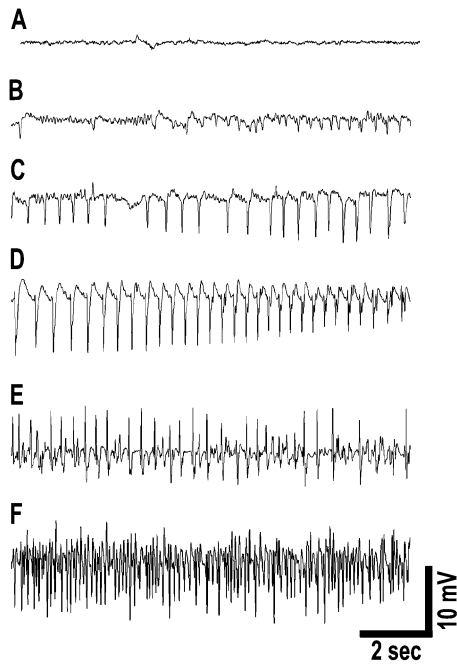


FIG. 2. EEG progression of DFP-induced SE. (A) Baseline activity prior to DFP injection. (B) Low-voltage fast activity appears within 2–3 min of DFP administration. (C) High-voltage slow activity appears within the next minute that progresses to (D) high-frequency and high-voltage spiking and (E and F) sustained continuous seizure activity. EEG activity at 15 min following DFP administration (F) demonstrates electrographic SE with fully developed continuous seizures. Spike frequency during SE was sustained at greater than 7–10 Hz. SE was induced by DFP within 7–8 min following injections. EEG activity correlated with behavioral observations.

Ca^{2+} indicator Fura-2 in acutely isolated hippocampal neurons from naive control, sham, and DFP-treated animals. Representative pseudocolor images of neurons from sham and DFP-treated animals are shown in Figure 3. Acutely isolated CA1 hippocampal neurons harvested from animals that underwent 1-h DFP-induced SE manifested mean $[\text{Ca}^{2+}]_i$ levels of $772.42 \pm$

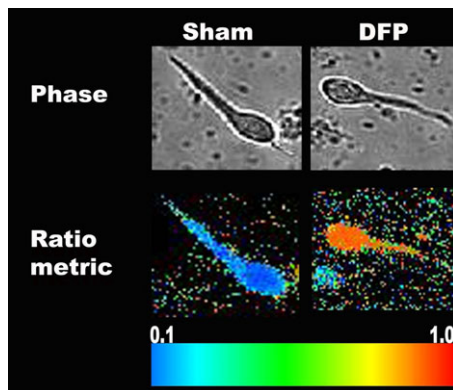


FIG. 3. Phase contrast and pseudocolor ratiometric images of representative sham- and DFP-treated neurons. Sham-treated neurons had bluish color that corresponds to lower Fura-2 ratio whereas DFP-treated neurons had orange-red color that corresponds to high Fura-2 ratio.

42.12nM, significantly ($p < 0.001$, one-way ANOVA, $n = 7$ animals) higher than $[\text{Ca}^{2+}]_i$ levels harvested from age-matched control ($248.12 \pm 23.12\text{nM}$, $n = 5$ animals) and sham animals ($251.66 \pm 30.04\text{nM}$, $n = 6$ animals, Fig. 4A). No significant differences were observed between the control and sham groups.

Analysis of the population distributions of $[\text{Ca}^{2+}]_i$ levels revealed only 7% of control neurons exhibiting $[\text{Ca}^{2+}]_i$ levels greater than 500nM with the majority of neurons in the lower range. In contrast, approximately 50% neurons from the DFP-treated animals had $[\text{Ca}^{2+}]_i$ levels greater than 500nM indicating a shift in the population of neurons to higher Ca^{2+} ratios (Fig. 4B). This rightward shift in distribution of $[\text{Ca}^{2+}]_i$ levels in DFP neurons was significantly different from control neurons (Fig. 4B, $p < 0.001$, chi-square test, $n = 150$ neurons). These experiments indicate that DFP-induced SE acutely increased $[\text{Ca}^{2+}]_i$ levels in hippocampal neurons.

Development of Calcium Plateau Following DFP-Induced SE

We next investigated the time course for the duration of elevated hippocampal neuronal $[\text{Ca}^{2+}]_i$ levels following DFP exposure. As shown in Figure 5, $[\text{Ca}^{2+}]_i$ levels were measured in CA1 hippocampal neurons at 1, 2, 7, 14, and 30 days after DFP-induced SE. $[\text{Ca}^{2+}]_i$ levels were $634.83 \pm 48.16\text{nM}$ ($n = 6$ animals) and $715.79 \pm 44.13\text{nM}$ ($n = 7$ animals) at 24 and 48 h following DFP-induced SE. At 1 week, $[\text{Ca}^{2+}]_i$ levels were still significantly elevated at $517.99 \pm 13.22\text{nM}$ ($n = 9$ animals). At 2 weeks after DFP-induced seizures, $[\text{Ca}^{2+}]_i$ levels were $385.08 \pm 32.15\text{nM}$ ($n = 7$ animals). At the end of 1 month following DFP administration, $[\text{Ca}^{2+}]_i$ levels were $378.06 \pm 46.21\text{nM}$ ($n = 6$ animals). At all these time points following DFP-induced seizures, $[\text{Ca}^{2+}]_i$ levels were significantly different from sham-treated $[\text{Ca}^{2+}]_i$ levels ($p < 0.001$, one-way ANOVA, Fig. 5). These experiments indicate that DFP-induced SE caused a Ca^{2+} plateau lasting for over a week.

Inhibition of Elevated Calcium Following DFP Administration by MK-801

Previous studies have implicated NMDA receptor system in mediating $[\text{Ca}^{2+}]_i$ elevations following central nervous system (CNS) injuries. We therefore investigated mechanism of Ca^{2+} entry by pretreating animals with MK-801 and then subjecting them to DFP-induced SE. As shown in Figure 6A, MK-801 pretreatment did not decrease the intensity or duration of DFP-induced SE. The MK-801-treated animals had comparable SE to untreated animals and required the same amount of diazepam to terminate SE. Thus, MK-801-DFP animals experienced the same degree of electrographic SE as the DFP alone treated animals.

However, MK-801 pretreatment significantly reduced the elevations in $[\text{Ca}^{2+}]_i$ levels that occurred in hippocampal neurons following DFP-induced seizures (Fig. 6B). Neurons isolated from animals pretreated with MK-801 manifested $[\text{Ca}^{2+}]_i$ levels ($284.06 \pm 26.64\text{nM}$) that were not significantly different from control animals ($251.84 \pm 18.56\text{nM}$) ($p = 0.08$, one-way ANOVA, $n = 5$ and 6 animals, respectively). These

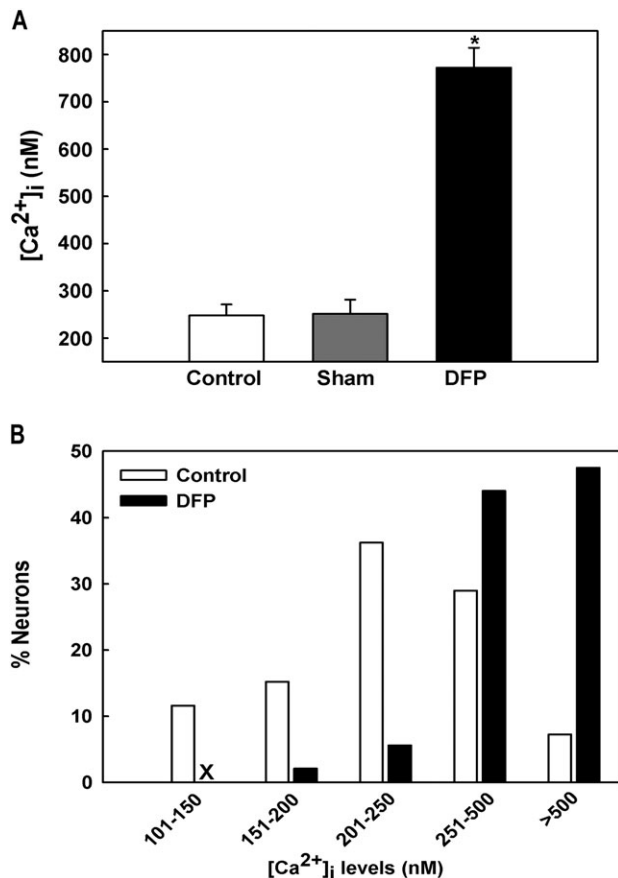


FIG. 4. Basal $[Ca^{2+}]_i$ in acutely isolated CA1 hippocampal neurons following DFP-induced SE. (A) Elevated $[Ca^{2+}]_i$ in CA1 hippocampal neurons acutely isolated from animals that had experienced 1 h of DFP-induced SE compared with neurons from control and sham-treated animals. (* $p < 0.001$, one-way ANOVA, *post hoc* Tukey test, $n = 7, 5,$ and 6 animals, respectively). Data are represented as mean \pm SEM. (B) Distribution of $[Ca^{2+}]_i$ levels for sham and DFP-SE hippocampal neurons. Sham neurons demonstrated a normal distribution for $[Ca^{2+}]_i$ levels with approximately 90% of neurons exhibiting $[Ca^{2+}]_i$ levels less than 500nM and only 7–10% neurons exhibiting very high $[Ca^{2+}]_i$ levels. In contrast, DFP-SE neurons demonstrated a rightward shift toward higher $[Ca^{2+}]_i$ levels with approximately 50% neurons exhibiting $[Ca^{2+}]_i$ levels greater than 500nM ($n = 150$ neurons for each condition).

experiments indicated that the majority of Ca^{2+} that enters the neurons following DFP-induced SE is mediated by the NMDA receptor and that activation of the NMDA receptor during SE plays an important role in the development of the Ca^{2+} plateau.

DISCUSSION

The results from our study demonstrate that we have developed a reliable model of DFP-induced SE that has a high survival rate and can be used to investigate the long-term neurological disorders that are associated with DFP toxicity. The SE produced in this model had both behavioral and electrographic similarities to the SE produced by exposure to nerve gas (McDonough and Shih, 1993). DFP has been used in the past to

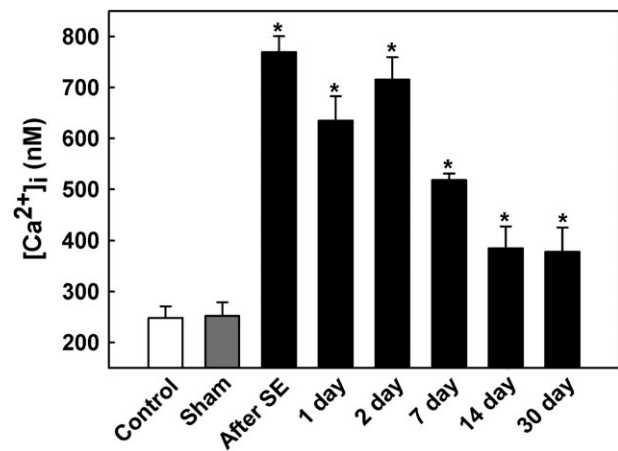


FIG. 5. Development of Ca^{2+} plateau following DFP-induced SE. CA1 hippocampal $[Ca^{2+}]_i$ in control (white bar), sham (gray bar), and DFP immediately after and 1, 2, 7, 14, and 30 days after SE (black bars). $[Ca^{2+}]_i$ in sham animals at each time point were not significantly different from the control values shown and thus were omitted from the graph for clarity. $[Ca^{2+}]_i$ in neurons isolated from DFP-SE animals was significantly higher than control and sham values (* $p < 0.05$, one-way ANOVA, *post hoc* Tukey test, $n =$ minimum of six animals at each time). Data are represented as mean \pm SEM.

induce motor convulsions and seizures (Kadriu *et al.*, 2009; Pibiri *et al.*, 2008; Tuovinen, 2004). To our knowledge, this is the first published study that has employed both Racine score and high-resolution EEG recordings to characterize the induction of SE in rodents following DFP administration. In addition, this study presents the first demonstration that DFP/OP compound toxicity can cause a prolonged Ca^{2+} plateau that may underlie some of the acute and long-term effects of OP toxicity on neuronal function and cognitive impairment.

Results demonstrated that reliable SE induction could be obtained by optimizing the vehicle, dose, and volume of DFP injections. DFP had a narrow dose range for producing SE without significant mortality. Mortality increased significantly when DFP dose exceeded 4 mg/kg. SE onset was very rapid when DFP was dissolved in ice-cold PBS solution compared with peanut oil or saline. Further, the volume of DFP injection was also critical to the success of the model. DFP injections with a volume between 250 and 300 μ l produced rapid onset of SE without significant mortality. Larger volume increased mortality in our study and a smaller volume did not reliably produce SE. The equilibration of DFP in the systemic space could possibly underlie the volume-dependent expression of DFP-induced SE and mortality. These findings are in agreement with those reported by Crawford *et al.*, (2004).

Another factor that significantly affected mortality was the dose of atropine. We found that a lower dose of atropine (0.2 mg/kg) administered after the DFP injection was not able to significantly lower the mortality. However, increasing the dose of atropine to 2 mg/kg allowed for greater than 90% survival after DFP-induced SE. Over 80% of the animals survived for more than 4 weeks at which point they were

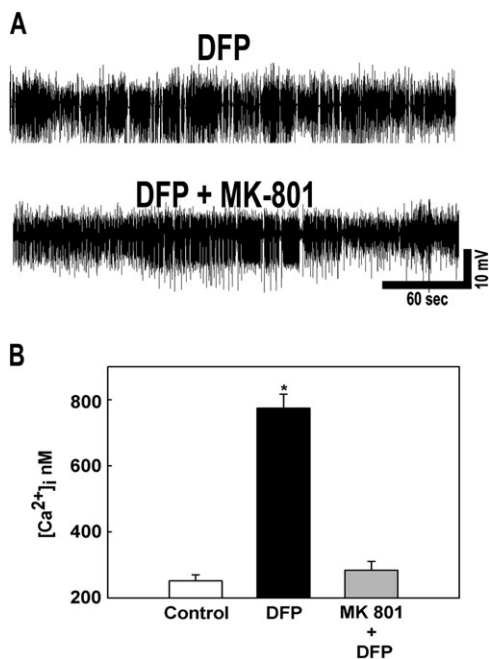


FIG. 6. Effect of MK-801 administration on DFP-induced SE. (A) Representative EEG pattern from animals pretreated with MK-801 and DFP alone. MK-801 pretreatment did not affect the severity, intensity, and duration of DFP-induced SE. (B) MK-801 pretreatment prevented the elevations in $[Ca^{2+}]_i$ that occur following DFP-induced SE. (* $p < 0.01$, one-way ANOVA, *post hoc* Tukey test, $n = 5, 7,$ and 6 animals, respectively). Data are represented as mean \pm SEM.

sacrificed for Ca^{2+} studies. Thus, our improved dose regimen of atropine, 2-PAM, and diazepam not only stopped DFP-induced SE but also protected a large number of animals from death. This model is ideally suited for studying the long-term effects of DFP-induced SE and provides a valuable tool in assessing the chronic effects of OP toxicity.

We have demonstrated that CNS injuries produce elevated $[Ca^{2+}]_i$ that persist for days following the initial seizure (reviewed in Nagarkatti *et al.*, 2009). This prolonged Ca^{2+} plateau coincides with the silent period of epileptogenesis and is an ideal substrate for inducing many of the long-term plasticity changes induced by brain injury. Evidence indicates that the Ca^{2+} plateau activates signaling cascades that are responsible for the ultimate expression of epilepsy (DeLorenzo *et al.*, 2005; Nagarkatti *et al.*, 2009). Acutely isolated hippocampal neurons from DFP-treated animals showed significant elevations in $[Ca^{2+}]_i$ levels that lasted for almost 2 weeks following the initial SE. One might argue that DFP-treated animals are in a state of chronic cholinergic overstimulation that could result in expression of Ca^{2+} plateau. In our model, animals were injected with oxime reactivator 2-PAM as a part of drug rescue regimen. Studies in the literature show that with oximes on board, DFP-inhibited AChE gets reactivated rapidly (Acharya *et al.*, 2009; Antonijevic and Stojiljkovic, 2007; Oh *et al.*, 2008). Using this procedure, in our model, all the signs of cholinergic overstimulation were gone by 3–5 h. The rescued animals recovered and resumed

normal activity within 1–2 days after DFP. Taken together, this indicates that the DFP-treated animals were not in a state of continual cholinergic overstimulation. Therefore, the observed Ca^{2+} plateau was arising from SE and not because of the prolonged cholinergic overstimulation. This is in agreement with development of Ca^{2+} plateau following pilocarpine-induced SE (Raza *et al.*, 2004). These elevations in $[Ca^{2+}]_i$ levels were mediated and maintained by Ca^{2+} entry from NMDA receptor system because pretreatment with MK-801 prevented the rise in Ca^{2+} levels without any effects on SE severity. The discovery that Ca^{2+} dynamics are altered following DFP-induced seizures is an important one because it provides for pathways that could be pharmacologically manipulated to provide neuroprotection following nerve agent exposure (DeLorenzo *et al.*, 2005; Filbert *et al.*, 2005).

Acute CNS injuries such as SE, traumatic brain injury (TBI), and stroke are all associated with increases in $[Ca^{2+}]_i$ in the immediate postinjury phase that lasts for days after the initial brain insult (Nagarkatti *et al.*, 2009). During this period, Ca^{2+} activates many signaling cascades and alters the synaptic plasticity such that the brain loses its functional balance between excitation and inhibition (DeLorenzo *et al.*, 2005). Indeed, these three brain injuries are among the most common causes of acquired epilepsy. These elevations in Ca^{2+} levels have also been implicated in neuronal death and cognitive deficits following brain injuries (Deshpande *et al.*, 2008; Sun *et al.*, 2008). Research into the genesis of this Ca^{2+} plateau has implicated NMDA receptor system because pretreatment with its antagonist MK 801 prevented the rise in Ca^{2+} levels following brain injuries and also prevented development of epilepsy (Raza *et al.*, 2004). In addition, NMDA receptor inhibition during SE and TBI also prevented behavioral and cognitive changes (Deshpande *et al.*, 2008; Rice *et al.*, 1998). Thus, inhibition of the Ca^{2+} plateau could potentially prevent the central aftereffects of DFP poisoning such as development of epilepsy and cognitive deficits. It will be interesting to investigate these possibilities in future studies.

Pilocarpine is a popular chemical used to induce SE and study acquired epilepsy in rodents. Its wide availability and ease of use has contributed to its popularity. This model has also been regarded as an alternative model to studying the molecular mechanisms of neuropathology and screening neuroprotectants following nerve agent exposure (Tetz *et al.*, 2006). However, this still represents an indirect approach to study effects of nerve agent intoxication. In this regard, DFP presents a better alternative. DFP not only shares many physical and kinetic properties with other nerve agents but also produces seizures by similar mechanism that is AChE inhibition. Our studies show that onset of seizure activity and spike frequency following DFP injection were faster than pilocarpine administration (data not shown) and resembled soman exposure (McDonough and Shih, 1993). Both pilocarpine- and DFP-induced seizures resulted in the development of Ca^{2+} plateau that was sensitive to NMDA antagonism. We EEG

monitored the animals for 24 h after the DFP-induced seizures were stopped with diazepam, and during this period, we observed no seizures. However, during the subsequent period ensuing to 30 days post DFP injections, the animals were not EEG monitored in this study. However, with DFP intoxication, the Ca^{2+} plateau produced was of a much longer duration than the pilocarpine-induced Ca^{2+} plateau (Raza *et al.*, 2004). This indicates that DFP-induced SE produced a more severe and longer lasting effect on the development of the Ca^{2+} plateau than that produced by pilocarpine and suggests that DFP intoxicated animals might have a shorter period of epileptogenesis and may develop epilepsy sooner compared with pilocarpine administration. These possibilities along with brain histopathological changes are actively being investigated by our laboratory. Thus, this DFP model of OP toxicity provides a SE model that mimics both acute and long-term behavioral and molecular effects of nerve agent exposure without having to rely on non-OP compound models.

FUNDING

This work was supported by the CounterACT Program, National Institutes of Health Office of the Director, and the National Institute of Neurological Disorders and Stroke [Grant Number UO1NS058213] to R.J.D. Its contents are solely the responsibility of the authors and do not necessarily represent the official views of the federal government. This study is also supported by National Institute of Neurological Disorders and Stroke [Grant numbers RO1NS051505 and RO1NS052529] to R.J.D.

REFERENCES

- Acharya, J., Gupta, A. K., Dubey, D. K., and Raza, S. K. (2009). Synthesis and evaluation of novel bis-pyridinium oximes as reactivators of DFP-inhibited acetylcholinesterase. *Eur. J. Med. Chem.* **44**, 1335–1340.
- Antoničević, B., and Stojiljković, M. P. (2007). Unequal efficacy of pyridinium oximes in acute organophosphate poisoning. *Clin. Med. Res.* **5**, 71–82.
- Auta, J., Costa, E., Davis, J., and Guidotti, A. (2004). Imidazenil: a potent and safe protective agent against diisopropyl fluorophosphate toxicity. *Neuropharmacology* **46**, 397–403.
- Bajgar, J. (2004). Organophosphates/nerve agent poisoning: mechanism of action, diagnosis, prophylaxis, and treatment. *Adv. Clin. Chem.* **38**, 151–216.
- Bouzarth, W. F., and Himwich, H. E. (1952). Mechanism of seizures induced by di-isopropyl fluorophosphate (DFP). *Am. J. Psychiatry* **108**, 847–855.
- Broomfield, C. A., and Kirby, S. D. (2001). Progress on the road to new nerve agent treatments. *J. Appl. Toxicol.* **21**(Suppl. 1), S43–S46.
- Coupland, R., and Leins, K.-R. (2005). Science and prohibited weapons. *Science* **308**, 1841.
- Crawford, S. M., Compton, J. R., Tetz, L. M., Ratcliffe, R. H., Steele, K. E., Gordon, R. K., and Nambiar, M. P. (2004). Development of a rat diisopropylfluorophosphate-induced seizure/status epilepticus model for screening of neuroprotectants following exposure to chemical warfare agents. Paper presented at the Scientific Conference on Chemical and Biological Defense Research, Hunt Valley, MD, A976944.
- DeLorenzo, R. J., Sun, D. A., and Deshpande, L. S. (2005). Cellular mechanisms underlying acquired epilepsy: the calcium hypothesis of the induction and maintenance of epilepsy. *Pharmacol. Ther.* **105**, 229–266.
- Deshpande, L. S., Sun, D. A., Sombati, S., Baranova, A., Wilson, M. S., Attkisson, E. A., Hamm, R. J., and DeLorenzo, R. J. (2008). Alterations in neuronal calcium levels are associated with cognitive deficits after traumatic brain injury. *Neurosci. Lett.* **441**, 115–119.
- Dingeman, A., and Jupa, R. (1987). Chemical warfare in the Iran-Iraq conflict. *Strategy Tactics Mag* **113**, 51–52.
- Eyer, P. (2003). The role of oximes in the management of organophosphorus pesticide poisoning. *Toxicol. Rev.* **22**, 165–190.
- Filbert, M., Levine, E., and Ballough, G. (2005). Neuroprotection for nerve agent-induced brain damage by blocking delayed calcium overload: a review. *J. Med. Chem. Biol. Radiol. Def.* **3** (online).
- Golomb, B. A. (2008). Acetylcholinesterase inhibitors and Gulf War illnesses. *Proc. Natl Acad. Sci. U.S.A.* **105**, 4295–4300.
- Gryniewicz, G., Poenie, M., and Tsien, R. Y. (1985). A new generation of Ca^{2+} indicators with greatly improved fluorescence properties. *J. Biol. Chem.* **260**, 3440–3450.
- Kadriu, B., Guidotti, A., Costa, E., and Auta, J. (2009). Imidazenil, a non-sedating anticonvulsant benzodiazepine, is more potent than diazepam in protecting against DFP-induced seizures and neuronal damage. *Toxicology* **256**, 164–174.
- Karalliedde, L., and Senanayake, N. (1989). Organophosphorus insecticide poisoning. *Br. J. Anaesth.* **63**, 736–750.
- Lemercier, G., Carpentier, P., Sentenac-Roumanou, H., and Morelis, P. (1983). Histological and histochemical changes in the central nervous system of the rat poisoned by an irreversible anticholinesterase organophosphorus compound. *Acta Neuropathol.* **61**, 123–129.
- Mark, A. B., and Kelley, A. B. (1998). Review of health consequences from high-, intermediate- and low-level exposure to organophosphorus nerve agents. *J. Appl. Toxicol.* **18**, 393–408.
- McDonough, J. H., Jr, and Shih, T. M. (1993). Pharmacological modulation of soman-induced seizures. *Neurosci. Biobehav. Rev.* **17**, 203–215.
- McDonough, J. H., Jr, and Shih, T. M. (1997). Neuropharmacological mechanisms of nerve agent-induced seizure and neuropathology. *Neurosci. Biobehav. Rev.* **21**, 559–579.
- Newmark, J. (2004). The birth of nerve agent warfare: lessons from Syed Abbas Foroutan. *Neurology* **62**, 1590–1596.
- Nagarkatti, N., Deshpande, L. S., and DeLorenzo, R. J. (2009). Development of the calcium plateau following status epilepticus: role of calcium in epileptogenesis. *Expert Rev. Neurother.* **9**, 813–824.
- Oh, K. A., Park, N. J., Park, N. S., Kuca, K., Jun, D., and Jung, Y. S. (2008). Reactivation of DFP- and paraoxon-inhibited acetylcholinesterases by pyridinium oximes. *Chem. Biol. Interact.* **175**(1–3), 365–367.
- Pibiri, F., Kozikowski, A. P., Pinna, G., Auta, J., Kadriu, B., Costa, E., and Guidotti, A. (2008). The combination of huperzine A and imidazenil is an effective strategy to prevent diisopropyl fluorophosphate toxicity in mice. *Proc. Natl Acad. Sci. U.S.A.* **105**, 14169–14174.
- Racine, R. J. (1972). Modification of seizure activity by electrical stimulation: II. Motor seizure. *Electroencephalogr. Clin. Neurophysiol.* **32**, 281–294.
- Raza, M., Blair, R. E., Sombati, S., Carter, D. S., Deshpande, L. S., and DeLorenzo, R. J. (2004). Evidence that injury-induced changes in hippocampal neuronal calcium dynamics during epileptogenesis cause acquired epilepsy. *Proc. Natl Acad. Sci. U.S.A.* **101**, 17522–17527.
- Rice, A. C., Floyd, C. L., Lyeth, B. G., Hamm, R. J., and DeLorenzo, R. J. (1998). Status epilepticus causes long-term NMDA receptor-dependent behavioral changes and cognitive deficits. *Epilepsia* **39**, 1148–1157.
- Rod, C. S. (2009). Status epilepticus in the developing brain: Long-term effects seen in humans. *Epilepsia* **50**(s12), 32–33.

- Shih, T. M., Duniho, S. M., and McDonough, J. H. (2003). Control of nerve agent-induced seizures is critical for neuroprotection and survival. *Toxicol. Appl. Pharmacol.* **188**, 69–80.
- Sun, D. A., Deshpande, L. S., Sombati, S., Baranova, A., Wilson, M. S., Hamm, R. J., and DeLorenzo, R. J. (2008). Traumatic brain injury causes a long-lasting calcium-plateau of elevated intracellular calcium levels and altered calcium homeostatic mechanisms in hippocampal neurons surviving the brain injury. *Eur. J. Neurosci.* **27**, 1659–1672.
- Tetz, L. M., Rezk, P. E., Ratcliffe, R. H., Gordon, R. K., Steele, K. E., and Nambiar, M. P. (2006). Development of a rat pilocarpine model of seizure/status epilepticus that mimics chemical warfare nerve agent exposure. *Toxicol. Ind. Health* **22**, 255–266.
- Tuovinen, K. (2004). Organophosphate-induced convulsions and prevention of neuropathological damages. *Toxicology* **196**, 31–39.
- Turski, W. A., Czuczwar, S. J., Kleinrok, Z., and Turski, L. (1983). Cholinomimetics produce seizures and brain damage in rats. *Experientia* **39**, 1408–1411.
- Wright, L. K., Liu, J., Nallapaneni, A., and Pope, C. N. (2009). Behavioral sequelae following acute diisopropylfluorophosphate intoxication in rats: comparative effects of atropine and cannabinomimetics. *Neurotoxicol. Teratol.* **32**, 329–335.
- Yokoyama, K., Yamada, A., and Mimura, N. (1996). Clinical profiles of patients with sarin poisoning after the Tokyo subway attack. *Am. J. Med.* **100**, 586.